

The Antenna Configuration of the Allen Telescope Array

Douglas Bock

Radio Astronomy Laboratory, University of California at Berkeley

January 8, 2003

ABSTRACT

This memo describes the antenna configuration of the Allen Telescope Array. In order to satisfy the complex and substantial site constraints it has been found expedient to optimize the antenna positions, rather than generating them from rules: the configuration is *defined* by the constraints and optimization method. Analysis of the configuration shows it will lead to an excellent synthesized beam, high-quality imaging, and be robust to antenna failure and antenna position errors. The final antenna configuration will have very similar performance and be presented in an addendum.

1. Introduction

The goal of this memo is to present the antenna configuration of the ATA, and to report on its design. Previous memos (Bock 2000, 2001a; Helfer 2001) described ways by which an antenna configuration for an instrument such as the ATA can be designed by rule, i.e. *generated*. Such an approach relies on the availability of a substantially unobstructed portion of land, so that the antennas may actually be placed at all (or almost all) the generated positions. At the Hat Creek Radio Observatory, existing constraints such as buildings, roads, rough ground, sensitive resources, and the desire to minimize the removal of trees make this approach undesirable. Configurations relying on this approach are substantially degraded by the absence of antennas from their ideal positions. For the ATA, it was decided to design the configuration by *optimizing* to achieve the desired uv distribution in the presence of the existing site constraints. As will be seen in this memo, this approach provides a substantially better result than those configurations previously described.

One consequence of the decision to optimize (rather than generate) the antenna configuration is that the configuration is in essence defined by the site constraints and optimization algorithm. Until construction is complete, the actual antenna positions will remain merely a snapshot reflecting the present knowledge of the exact site constraints. However, these constraints are now fairly stable: the limited refinements still required will not alter the configuration's ability to satisfy the scientific objectives. The final antenna positions will be reported once construction of the foundations is complete.

In the following, the scientific objectives and parameters of the the configuration are first presented, followed by a description of the configuration optimization and an analysis. The detailed site constraints are relegated to an appendix.

2. Scientific objectives

The scientific objectives of the ATA, as they apply to the configuration design, were considered in Bock (2001b). Two key scientific areas for the ATA were identified: wide-area surveys and time-domain studies. The first of these drive the configuration design, requiring:

- excellent sensitivity from from DC to $70''$ (at 1.4 GHz)
- a high-quality beam for long tracks
- a high-quality snapshot beam (this satisfies the previous point, and makes scheduling easier)
- low sidelobes
- limited shadowing at the Galactic Center.

The last two points additionally satisfy the requirements for time-domain studies, including SETI. The high-quality beam is taken to mean an approximately round Gaussian. Since the discussions reported in Bock (2001b), a general consensus was reached that the beam should be round at $\delta = 10^\circ$, as a balance between reducing beam elongation at low declinations and retaining brightness sensitivity at high declinations.

3. Configuration optimization

Several methods have recently been developed for configuration optimization. The three considered here were developed by Keto (1997), Kogan (1999), and Boone (2001), the latter two for the ALMA configuration design. The Keto method uses a Kohonen self-organizing neural network algorithm. The principal concern from the ATA standpoint is the speed of the algorithm: it is unwieldy for more than about 50 antennas. This method was used for early ($N \sim 50$) studies, and then not further. Kogan’s method was applied to a complete ATA configuration optimization. This method uses an analytic solution to determine the antenna movements necessary to improve the synthesized beam at a given point. Large near-in sidelobes are attacked in turn, producing a round beam with very low inner sidelobes (within approximately the inner N beam areas). Unfortunately this method does not constrain the size of the uv distribution, so it is not possible to set the size

of the synthesized beam.¹

The final method (Boone 2001) works on the uv samples involving each antenna in turn, calculating the gradient required to “correct” to the desired distribution the uv density at the location of each uv sample. The antenna move is the vector average of these gradients. Thus the move calculation is $O(N)$ and the entire optimization is $O(N^2)$ per iteration. Since the algorithm produces acceptable results quickly (16 iterations over approximately two hours) it is reasonable for ATA snapshot optimization. This method has been used for all recent configuration designs for the ATA, including for the configuration presented in this memo.

3.1. Application to the ATA

Boone has implemented his optimization in a C++ library (named “APO”). The version of the code used for the ATA configuration design was that dated September 2000, with a few alterations to reduce the running time and to correct a minor bug related to validating the initial antenna positions. The code allows the desired uv distribution to be specified by a truncated Gaussian, while constraining the antenna positions to areas defined by a mask (a FITS file), and to specified minimum and maximum baseline lengths. For the ATA, the mask was generated to satisfy numerous site constraints; full details of these are given in appendix A. Iteratively it was determined that an area of trees near the center of the array would need to be removed to satisfy the objectives (as judged by convergence of the algorithm). The `miriad` script used to create the fits mask takes inputs of “in” and “out” polygons described in text files; it could have application in other projects.

Choice of the uv distribution As discussed in section 2, the ATA was specified to have a round Gaussian beam, implying that the uv distribution should have a Gaussian density profile. The Gaussian 1-D profile was chosen to have a FWHM of 500 m, experimentally the maximum that could be fitted on the site (i.e., choosing a larger FWHM precluded convergence of the algorithm). The resulting configuration thus has the highest resolution ($78''$ at transit for $\delta = 10^\circ$) that the site will allow while retaining the excellent sidelobe performance provided by this method of configuration design. Note that a higher resolution would have been possible with a configuration weighted more uniformly, but the result would have been higher sidelobes. The maximum baseline in the model was set at 500 m, i.e. the model was truncated at this value. The exact value of this parameter did not seem to have much effect given the specified FWHM and site constraints. The actual maximum baseline in this configuration is 913 m, although there are very few baselines around this length. The complete inputs used to generate the final configuration are given in table 1.

¹In studies for the VLA E-array effective use of Kogan’s method has been made by confining the antennas to a small area; applied to the ATA this would yield an approximately uniform distribution of antennas, with a corresponding increase in near sidelobes.

file contents	line number	notes
350 / nb of antennae	2	
1 / nb of conf	3	we have only one configuration
0 / nb of common ant	4	irrelevant for single configurations
122150 / nb of visibilities	5	
40.8 / site latitude	6	
0.05 / opacity	7	irrelevant for snapshot optimizations
10.0 / source declination	8	
0.0 / initial hour angle	9	
0.10 / integration time	10	i.e. one instantaneous sample only;
0.10 / hour angle sample interval	11	length does not affect the optimization
900.0 / maximal baseline	12	maximum allowable
500.0 / max baseline for model	14	maximum in the target uv distribution
6.1 / diameter	15	
10.8 / minimum distance between antennas	16	
8.0 / minimum baseline	17	minimum projected baseline
10.8 / min baseline for model	18	
o1.fits / name of map file	22	
0.50 / x pixel size of map	23	in meters
0.50 / y pixel size of map	24	
425.0 / x center of map	25	distance of the coord. origin from left
330.0 / y center of map	26	distance of coord. origin from bottom
500.0 / fwhm of model	27	fwhm of model uv distribution
1 / map as background	28	

Table 1: The input file for the optimization. Obsolete inputs have been omitted.

Running the algorithm After 16 iterations of the algorithm, the configuration was no longer changing substantially, and the optimization was stopped. The resultant configuration is overlaid on the mask used to constrain it in figure 1. Note that the configuration is centrally condensed overall, as expected from the Gaussian uv distribution required. Also note that the antennas are pushed up against several boundaries: near the center of the array, these are a portion of the trees near the main laboratory building, the observatory road, and lava flow edges. These limits constrain the level of the near sidelobes. Given all the other unavailable land near the center of the array, it was necessary to include a portion of the tree-covered area (about half) to get the algorithm to converge. Antennas are also pushed up against the eastern, southern and western edges of the site: these limits constrain the resolution and the shape of the beam (we could have had a slightly nicer beam with an array of lower resolution). The antenna positions are given in the file `config_o3_1.txt`, an attachment to this memo. The file lists the topocentric antenna coordinates in meters relative to the origin specified in the APO input file above, with north before

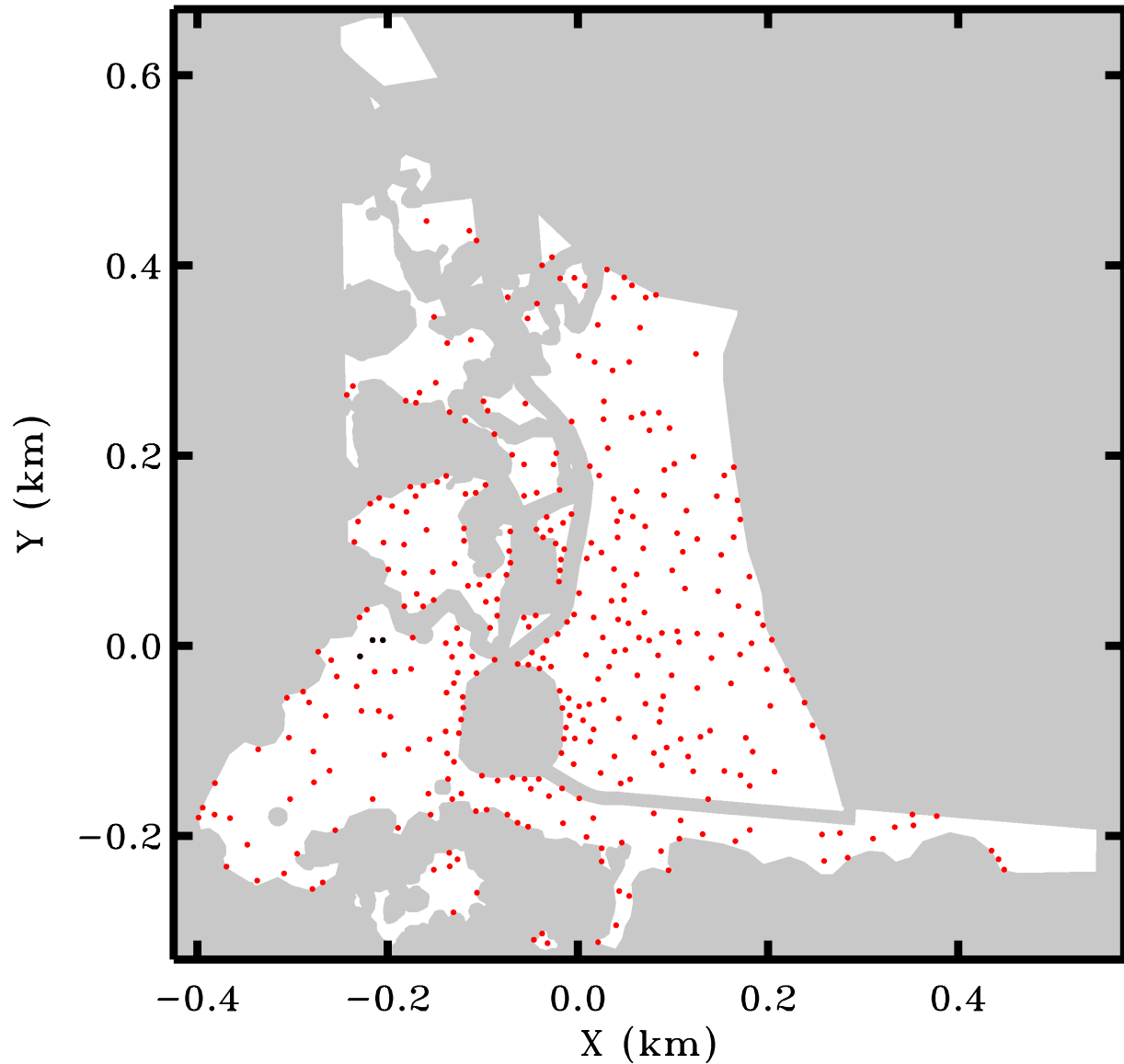


Fig. 1.— ATA antenna positions overlaid on the site mask used for configuration design, with a resolution of 0.5×0.5 m (PTA antennas are colored black).

east.² This is the format expected by `miriad` with `baseunit=-3.33564`. The first three antennas listed are those in place as the Production Test Array.

The algorithm is somewhat sensitive to the starting point. Small changes of ~ 100 m in the center of the initial distribution (lines 25 and 26 in table 1) resulted in a similar bias in the

²The coordinate system is actually based on NAD 1927 (CONUS), with the local origin UTM N4519514 E629344 Zone 10N, i.e. the coordinate system is rotated 1° east of true north.

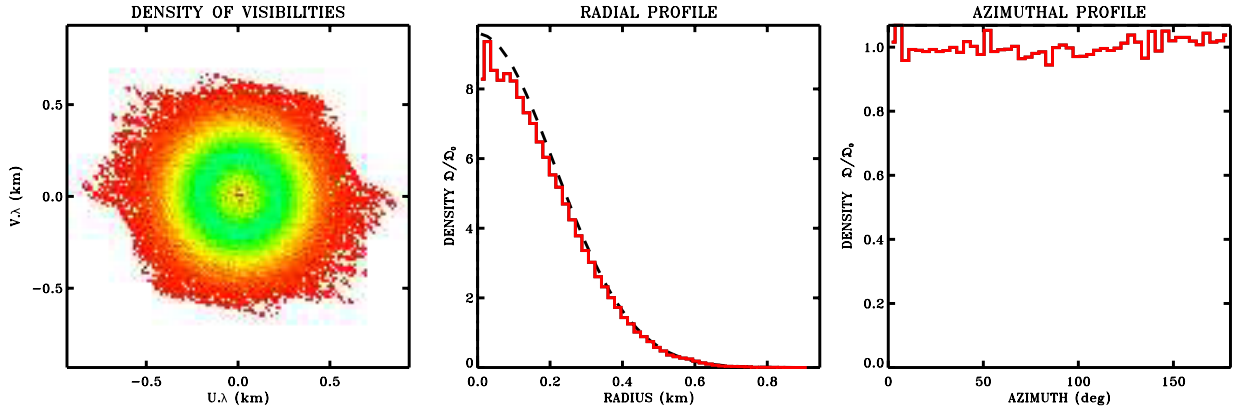


Fig. 2.— Uniformity of the uv samples

optimized array, and hence in a slightly poorer beam. The situation generally improved with further iterations. However, when the initial antenna distribution was centered far from the center of the site, the configuration did not appear to converge in a reasonable number of iterations. Thus it appears necessary to start with a “reasonable” configuration when doing the optimization. Note that the code first moves any antennas that begin outside the allowed areas to legal positions.

Some trial and error in finding the starting conditions is needed to determine the size of the array that can be fitted on a given site. Once reasonable starting conditions are found, alternate similar solutions can be found with minor changes in the initial conditions. This result could imply insufficient iterations for complete convergence, or the presence of several local minima in a broad overall solution minimum.

4. Analysis

The degree to which the optimization has succeeded can be seen from a plot of the density of uv samples (figure 4). The distribution is azimuthally symmetric; radially it closely approaches the desired Gaussian. However, the real test is the quality of the corresponding beam.

4.1. The synthesized beam

The synthesized beam has been calculated using standard `miriad` analysis tasks, and is shown in figure 3. It is clear that the beam is of very high quality, a result of the large N design and the freedom the antennas have to move during the optimization. The near-in sidelobes (within the inner N beam areas) are all less than 1%. The beam is round and near-Gaussian, as demonstrated by the low residuals after subtraction of a best fit Gaussian. Looking further from the beam center

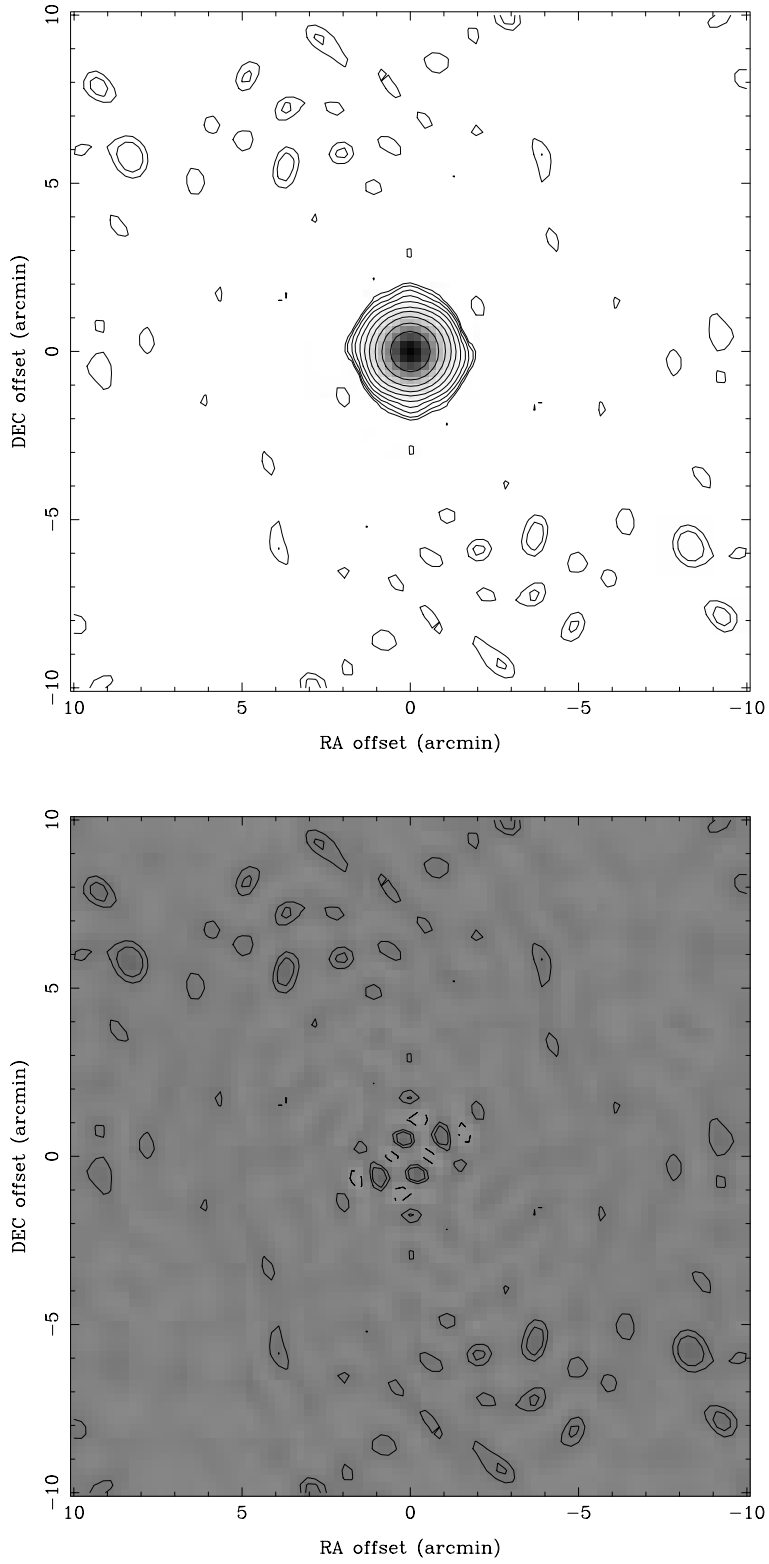


Fig. 3.— Inner region of the synthesized beam at 1.4 GHz (top), and residual after subtraction of a Gaussian model (bottom). Contours for both images are logarithmic starting at ± 0.5 , ± 0.9 , $\pm 1.6\%$

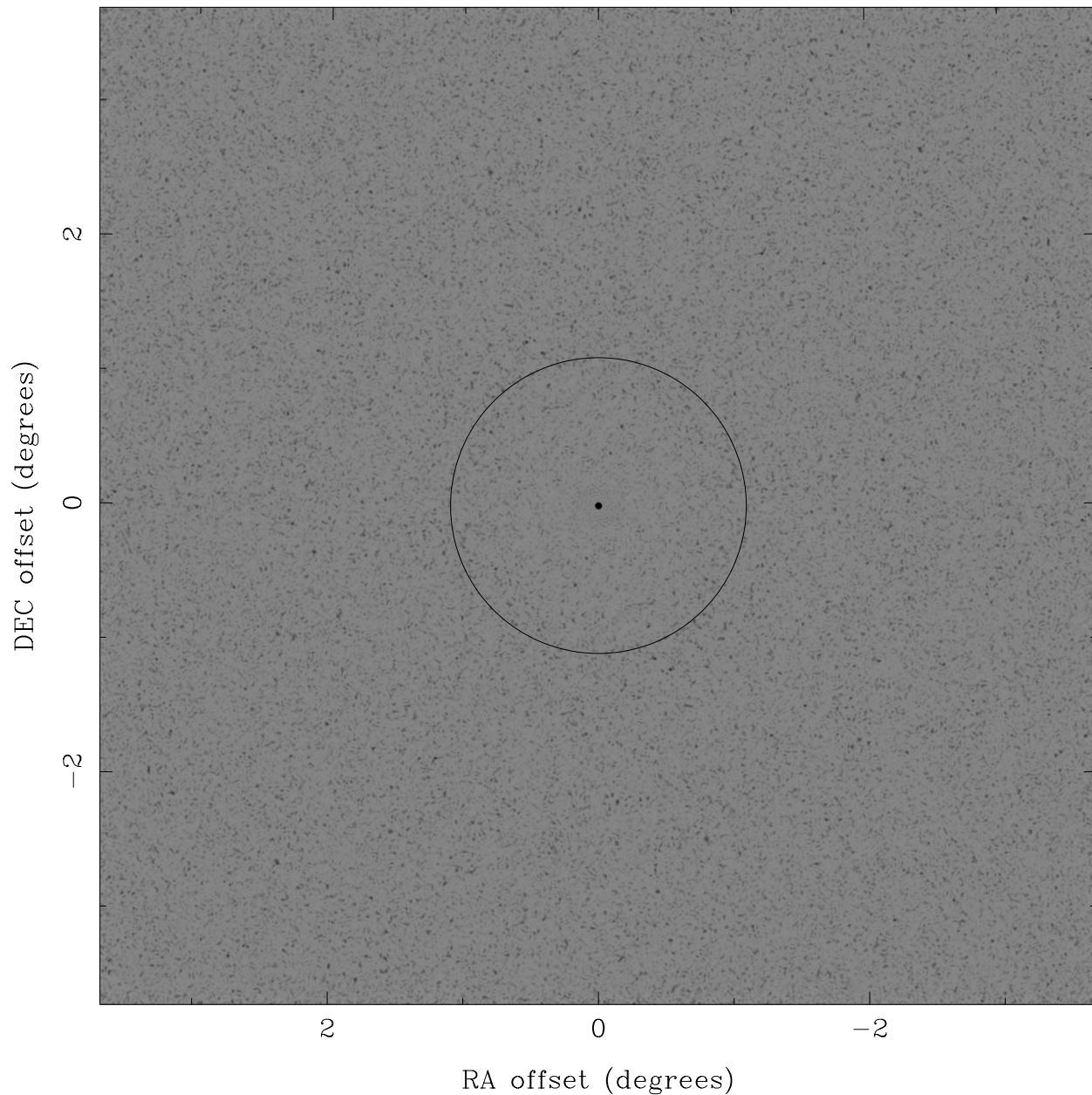


Fig. 4.— Synthesized beam over the area of the primary beam at 1.4 GHz (FWHM shown as a circle), with the grayscale saturated at $\pm 5\%$

(figure 4), we see that the sidelobes over all have a uniform character. There are no grating lobes present. Beyond approximately the inner N beam areas the sidelobe response is dominated by the value of N rather than the individual arrangement of antennas, since the antennas are pseudo-random. The sidelobe “noise” is 0.3% (rms), $\sim 1/N$. Individual sidelobes can be much higher, up to several percent (figure 5). Many of these sidelobes will be substantially attenuated by the

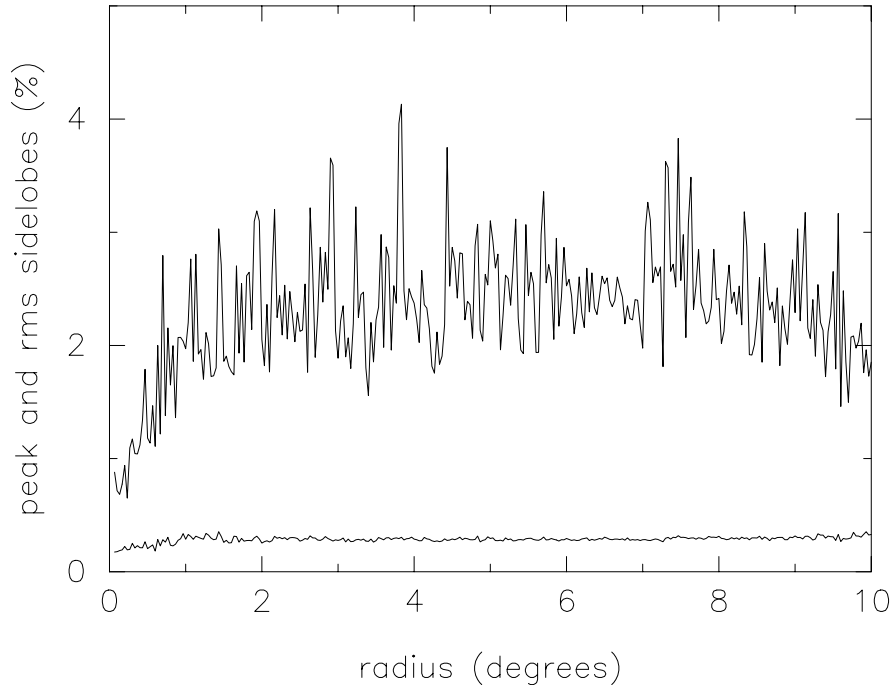


Fig. 5.— Plot of the sidelobe statistics (at 1.4 GHz), showing the peak (upper curve) and average sidelobe magnitude in annuli of $120''$. Note that the sidelobes will be substantially attenuated beyond the edge of the primary beam (radius 1.25° at 1.4 GHz).

antenna primary beam. Additional algorithms (e.g. Woody 2001) may be used to reduce the peak sidelobes substantially with small motions of antennas. These can be applied either to all sidelobes or, with better effect, just to those sidelobes within the primary beam.

There may be circumstances for which a still rounder beam, with even lower sidelobes, is desired. One possible reweighting scheme (applying a uniform weighting and tapering) reduces the near sidelobes to less than 0.1% with a 10% penalty in sensitivity. It would be desirable to develop more sophisticated reweighting schemes for large- N arrays to deal with the tradeoffs between beamshape, sensitivity, and interference mitigation. Used independently, interference mitigation schemes may increase the sidelobes.

Effect of longer tracks The sidelobe levels may be reduced further with long tracks. For example, the synthesized beam for an 8-hour track consisting of 80 snapshots has far sidelobes (both peak and rms) reduced by about a factor of 10. The peak near sidelobes are also reduced, by a factor of about 3.

Declination effects As mentioned above, the configuration was optimized to give a snapshot beam of $78'' \times 78''$ at $\delta = 10^\circ$. The beam will be smaller at the zenith and larger at the lowest

Declination	Beam (R.A. × Dec.)
90	78'' × 100''
60	78 × 71
45	78 × 67
40.8	78 × 67
30	78 × 68
15	78 × 74
10	78 × 78
0	78 × 89
–15	78 × 119
–30	78 × 204

Table 2: Size of the synthesized beam (natural weighting) for snapshot observations made on the meridian

declinations. For snapshot observations on the local meridian, the beam will be $78'' \times 67'' \sec(\delta - 40.8^\circ)$. The beams for various declinations are given in table 2. As long as there is no shadowing, the beamshape (including sidelobes) stays the same with this foreshortening, irrespective of azimuth.

4.2. Expected imaging performance

The large- N design, which offers excellent snapshot imaging within a large primary beam, will make the ATA a premier imaging instrument. Some parameters of the ATA relevant to imaging are listed and compared to those of the Very Large Array in table 3. On the basis of line mosaicing speed, the ATA will be substantially superior to the VLA.

The filling factor It has recently become common to use a parameter known as the *filling factor* to compare the brightness sensitivity of interferometers. This is the degree to which the array is filled compared to a single dish of the same collecting area, a quantity which is well-defined only when the antennas are uniformly distributed within a circular area. A comparable parameter is the ratio of the area of the naturally weighted synthesized beam (at the zenith) to the beam area of a single dish of the same collecting area:

$$\Gamma = \left(\frac{2D\theta_i}{1.02\lambda} \right)^2 \frac{N}{\pi},$$

where the array consists of N elements of diameter D , and θ_i is the FWHM size of the synthesized beam at wavelength λ . For the well-defined case described above (and for similar antenna illumination all around), this is the same as the filling factor. Γ for the ATA is compared to the VLA in table 3.

	ATA	VLA D config.	VLA E config.
ND (mosaicing speed)	2135	675	675
Γ (\sim filling factor)	0.045	0.011	0.24
$ND\Gamma$	96	7	164
Shortest baseline	10.8 m	35 m	35 m
Spatial dynamic range	55	54	8.0
Snapshot near sidelobes (peak)	0.9%	30%	7%
Snapshot far sidelobes (rms)	0.3%	3.5%	3.7%

Table 3: Comparison of selected ATA imaging parameters to those of the Very Large Array in the D configuration and in the proposed E configuration. Note that the comparison does not take into account specific antenna optics, receiver noise, or bandwidth differences.

The ATA remains competitive overall even when imaging the most extended emission to which the proposed VLA E configuration would be sensitive. Yet the ATA will have substantially shorter minimum baselines, lower sidelobes, and less shadowing. Simulations of the performance of the ATA when observing extended complex regions have been made by Wright (2002).

The need for deconvolution The high-quality beam of the ATA will make deconvolution unnecessary when observing sources with a signal to noise below about 100. For other projects, visibility reweighting may be a useful alternative to deconvolution. If the uv data are truncated at a maximum baseline of 440 m, every uv cell will be filled. Reweighting can thus provide a “perfect” beam at some loss of sensitivity and resolution.

Optimizing the uv distribution to a Gaussian naturally fills the uv cells as evenly as possible. It would be possible to optimize the antenna configuration for longer tracks, rather than snapshot observations. The analysis of Boone (2002) shows that if the ATA configuration were optimized for 6-minute observations all uv cells of the array would be filled. Optimizations for tracks of varying lengths would take substantial computing resources and could possibly reduce the snapshot performance. However, as noted in section 4.1, longer observations made with snapshot-optimized beams already provide substantial benefits. During any track of several minutes or longer the uv cells will essentially all be filled.

4.3. Shadowing

Because the antenna geometry does not allow extremely short spacings (the shortest is $1.77D$), and because the array is relatively sparse, shadowing is not severe. In a two-hour observation of the Galactic Center, approximately 15% of correlations would be shadowed. this number is relatively sensitive to the exact details of the configuration: small variations have produced values of up to 20% for this parameter.

No attempt to reduce the shadowing of the antennas by each other has been made. Since this analysis has assumed the antennas are coplanar, any reduction of shadowing at low elevations would lead to a loss in critical short spacings at higher elevations. One could in principle design an array with no very short spacings (and hence no shadowing) and observe always at low elevations, but that would imply severe and probably intolerable scheduling constraints, and is effective in one dimension only. Other approaches include placing some antennas on angled platforms, or using topographical features to provide low-elevation coverage to the south. The former would add substantial cost, while the latter would reduce shadowing only slightly, while complicating the design substantially.

4.4. Tolerance to antenna failures

An important characteristic of the ATA (as with all large- N designs) will be its resistance to component failure, i.e. its ability to provide useful results in the presence of reasonable numbers of failures among the large- N part of the system. The configuration presented here preserves this characteristic: the random removal of 10% of the antennas increases the sidelobes only to about 2%, and adequately preserves the round beam. Correspondingly, this tells us that it would be of limited benefit to optimize for sidelobes (and beamshape deviation from the ideal Gaussian) much below 1%, since some antennas will always be out of action, slightly corrupting the ideal distribution.

4.5. Tolerance to antenna location errors

During the construction process, certain antennas in the lava flows will need to be moved slightly to avoid voids, cracks, etc. Furthermore, the optimization used for the antenna configuration is two-dimensional, while the site elevations actually vary by several meters. However, when random (x, y, z) position errors of $(1, 1, 2)$ m (rms) were added to the antenna positions, no appreciable changes in beamshape or sidelobe levels were detected. So the existing design is sufficient in these circumstances.

5. Discussion

5.1. Increasing the short spacings

There has recently been renewed interest in improving the ATA's short spacing coverage in order to image the most extended structures, by including baselines shorter than those that avoid collisions ($1.77D$). A small number (a few 10s) of closely-spaced antennas could add this capability to the ATA at appropriate sensitivity. Such an approach would necessitate software and/or hardware anti-collision systems, adding construction and operational complexity. It has been asserted

that software anti-collision systems could be designed that would avoid the need for hardware anti-collision systems, and even that hardware collisions would not be a concern. However, both these points need still to be demonstrated, and the overall costs compared to the scientific benefit of the additional shorter spacings. Studies to quantify the advantages to ATA imaging projects of adding shorter spacings and/or single-dish data are currently underway. One additional point needing investigation is whether crosstalk between antennas will be a problem at the shortest baselines.

5.2. Comparison to alternative configuration options

It is instructive to compare the configuration presented here with some alternative options. One possibility would be an array with the highest brightness sensitivity that maintains low far sidelobes (i.e. that avoids any regularly recurring the baselines). Such a configuration was presented in Bock (2001a). This compact configuration has a beam of about $150''$ (1.4 GHz) and near sidelobes of around 5%. In a two-hour transit-centered observation of the Galactic Center 59% of the correlations would be shadowed.

Another design investigated placed 200 antennas in a compact centrally condensed distribution and placed the remaining 150 antennas to optimize the overall array for higher-resolution imaging. In this design, the beam using just the inner 200 antennas is $156'' \times 153''$ with sidelobes of 1%. But the beam from the overall configuration has an ugly plateau with central peak, corresponding to the bimodal distribution of antennas. The resulting sidelobes are 1.6%, with a beam (poorly fit by a Gaussian) of $90'' \times 85''$.

I wish to thank Melvyn Wright for substantial help and encouragement, and Frederic Boone for making his code available.

REFERENCES

- Bock, D. 2000, *50-antenna sample configurations for the Allen Telescope Array*, ATA Memo 21.
- Bock, D. 2001a, *350-antenna sample configurations for the Allen Telescope Array*, ATA Memo 15.
- Bock, D. 2001b, *Allen Telescope Array RAL Configuration Science Requirements*, ATA Memo 20.
- Boone, F. 2001, *A&A*, 377, 368.
- Boone, F. 2002, *A&A*, 386, 1160.
- Helfer, T. T. 2001, *Notes on Configurations for the ATA*, ATA memo 32.
- Keto, E. 1997, *ApJ*, 475, 843

Kogan, L. 1999, *PASP*, 111, 510.

Woody, D. 2001, *Interferometer Array Point Spread Functions II. Evaluation and Optimization*, ALMA memo 390.

Wright, M.C.H. 2002, *Allen Telescope Array Imaging*, ATA memo 52.

A. The site constraints

The constraints here are those known as of the date of this memo. However, the configuration analyzed above (o3_1), as discussed previously, has been held stable for the last six months in order to allow consistent analyses. The most significant changes to the constraints since the above mask was created are that the main laboratory building is now expected to be retained, and that allowances have been made to protect a substantial portion of the plant *Iliamna bakeri*. The configuration has been reoptimized to take these changes into account, and the results show only a very slight decrease in the quality of the inner beamshape. The inner sidelobes remain below 1%. Further changes will come as a result of a more accurate characterization of the road and building locations, and during construction, when certain positions may be found geologically unsuitable.

The antennas The antennas trace out a sphere of radius 4.95 m from their elevation axis (0.25 m off the azimuth axis, at height 4.65 m). Their maximum height is 9.0 m (29.5 ft). A clear avenue of width 2 m (6.5 ft) below 2 m height may be found even between antennas pointed at each other (figure A), so typical passenger and small utility vehicles can pass through. Passage of large vehicles (or antennas) will require closely-spaced antennas to be pointed away, or often merely to be pointed in the same direction. The minimum spacing of well-placed antennas would be 10.4 m; the design minimum spacing is 10.8 m to allow for placement errors. The foundations will be within a radius of 1.36 m (4.5 ft), consisting of three 0.3-m diameter piers on a radius of 0.91 m. The configuration will not be designed specifically to avoid shadowing, since that would affect the short spacings at other elevations. Avoidance of shadowing by other objects is for elevation, $\mathcal{E} > 15^\circ$, unless otherwise specified. **The constraints discussed below are always by reference to the center of the antenna.**

The beam A transit synthesized beam of 78'' with near sidelobes under 1% is possible at small positive declinations using these constraints. The beam has been set to be round at transit for a declination of 10° , and is thus elongated at other declinations and hour angles.

The canal A new fence has been constructed 6–7.5 m from the canal, as required by the lease (figure A). Trees will be planted along the fenceline. The antennas will be placed at least 13.8 m from the fenceline, thus ensuring there is no shadowing at elevations less than $\mathcal{E} = 30^\circ$. The trees are to the north-east of the array, so this elevation limit will rarely be a problem. This scheme also allows passage between the trees and the antennas.

The road to the main lab Antennas are to be at least 8.5 m from the center of the road. Thus an antenna (or other load < 6 m wide) can be driven down the road without interrupting operations.

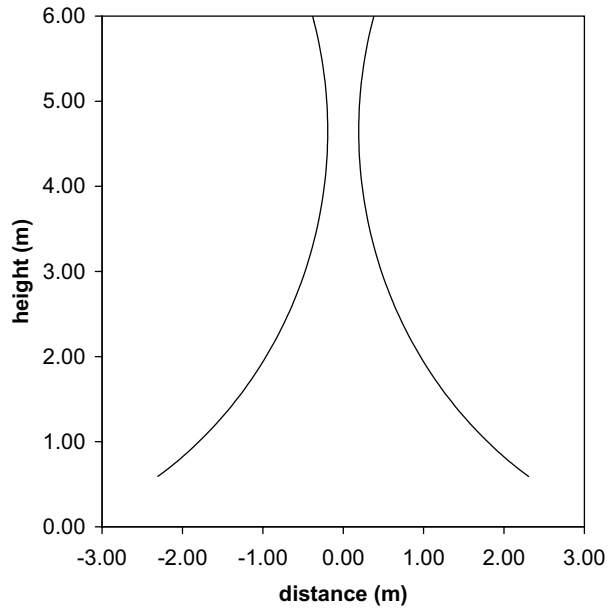


Fig. 6.— The clear space between antennas at a separation of 10.8 m

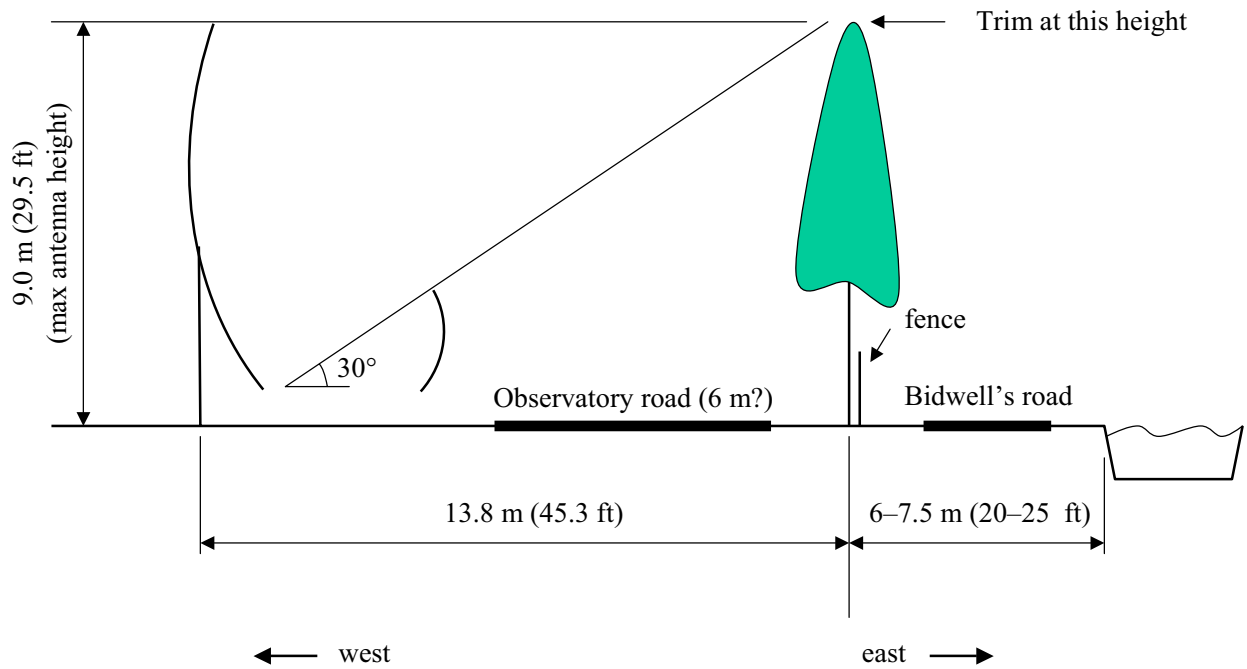


Fig. 7.— East-west profile showing the layout of roads, trees, antennas, fence, and the canal

The main lab To be retained, including existing road access and most parking. Antennas will not be shadowed by the main lab.

Labs 1 and 2 To be removed.

Pump room/well in meadow To be retained; antennas to avoid being shadowed.

BIMA antennas and infrastructure All to be removed or ignored, including antennas, underground fiber/coax/power on the T and to east/west arms, pit boxes, runways, and phase monitor. Antenna foundations can be partly on/off the T; they can be rotated so as to avoid drilling on the edge of the T.

Benchmarks at north and west ends of the T Antennas not to be placed within 10 m of these. Although placed by the USGS, these benchmarks are no longer active, so a more generous allowance is probably not necessary. No antennas are in the vicinity of the active bench mark on the lava (HAT CREEK NCMN D).

The backup generator To be retained in its present position; antennas avoid collision or being shadowed, but no other constraint. Note that the generator does not maintain observing capability in the absence of utility power, but sustains systems (e.g. cryogenics) that need power when observing is suspended. Thus RFI emissions are not a concern.

Gasoline storage tank To be moved to the new shop area.

Overhead utilities Main site power and telephone from BIMA station 2700N to the main lab to be placed underground (route to be decided after configuration is finalized, i.e. when designing new trenching). Power lines to east arm to be removed.

Underground utilities Power to pump house to be relocated along water line path to lab 1. Three underground power lines (from pumphouse, lab 1, last overhead pole) to gasoline storage tank to be removed. All others to be retained in their present positions except as described under *BIMA antennas and infrastructure* above.

Trees near the main lab About half the area of trees to the east of the main lab would be retained; antennas will not be shadowed by these above $\mathcal{E} = 30^\circ$, except on the south side of the trees, where some antennas could be shadowed below $\mathcal{E} = 45^\circ$ when looking north.

Other trees To be removed as necessary to prevent shadowing.

The Forest Service It is assumed the Forest Service will allow all positions which are either not in the roadless area, or which are within the roadless area but on the level meadow. There are relatively few trees on the Forest Service land, so it should be possible to retain these if they wish it.

Baker’s globe mallow (*Iliamna bakeri*) Where a group of this species occurs at the edge of the lava flow, and hence near the edge of the current mask, the mask has been altered to preserve that group to be 4 m distant from antenna centers. There are a few areas which take up substantial portions of real estate but have a low density of plants: the mask has not been altered, and some of these plants may be disturbed.

Prehistoric archaeological sites Apart from one underground power line, all construction will remain either on lava flows or at least 15 m away from prehistoric sites (30 m on National Forest lands). An archaeologist will monitor construction with 30 m of identified sites.

Historic archaeological site This site is an old dump near the canal. It will be possible to build over it.

The lava Lava to the north of the meadow to be used as necessary. Lava to the south to be used only if it improves the configuration performance once all other constraints have been taken into account.

Trenching The cost of trenching in uniform ground is not very sensitive to the configuration, so it has not been used as a constraint on the configuration. The cost of trenching is higher in lava than in alluvium; the foundation cost is somewhat reduced. However, to simplify the optimization, these cost considerations have not been taken into account. Further, note that most antennas are on alluvium.